DMD Fast Forward. Published on August 29, 2023 as DOI: 10.1124/dmd.123.001412
This article has not been copyedited and formatted. The final version may differ from this version.

Title Page

Potentiation of the Uricosuric Effect of Dotinurad by *Trans*-Inhibition of the Uric Acid Reabsorptive Transporter URAT1

Kazuki Fujita, Qiunan Zhu, Hiroshi Arakawa, Yoshiyuki Shirasaka, Ikumi Tamai

Faculty of Pharmaceutical Sciences, Institute of Medical, Pharmaceutical and Health Sciences, Kanazawa University

DMD Fast Forward. Published on August 29, 2023 as DOI: 10.1124/dmd.123.001412
This article has not been copyedited and formatted. The final version may differ from this version.

Running Title Page.

a) Running title:

Trans-inhibition of uric acid transporter URAT1 by dotinurad

b) Corresponding Author

Ikumi Tamai, Ph.D.,

Faculty of Pharmaceutical Sciences, Institute of Medical, Pharmaceutical and Health Sciences, Kanazawa University

Kakuma-machi, Kanazawa 920-1192, Japan.

Tel: +81-76-234-4479; Fax: +81-76-264-6284

Mail: tamai@p.kanazawa-u.ac.jp

c) Number of text pages: 42

Number of tables: 2

Number of figures: 5

Number of references: 20

Number of words in:

Abstract: 247

DMD Fast Forward. Published on August 29, 2023 as DOI: 10.1124/dmd.123.001412
This article has not been copyedited and formatted. The final version may differ from this version.

Introduction: 750

Discussion: 1493

d) A list of nonstandard abbreviations

IC_{50}: half maximal inhibitory concentration

NA: nicotinic acid

OAT: organic anion transporter

UA: uric acid

ULT: urate-lowering therapy

URAT1: urate transporter 1

DMD Fast Forward. Published on August 29, 2023 as DOI: 10.1124/dmd.123.001412
This article has not been copyedited and formatted. The final version may differ from this version.

Abstract

URAT1 is a transporter responsible for uric acid (UA) reabsorption by renal proximal tubules and a pharmacological target of uricosuric agents. Probenecid and benzbromarone have been used as uricosuric agents, while dotinurad was recently approved in Japan. Notably, the *in vitro* inhibition potential (IC_{50}) of dotinurad on URAT1 is not strong enough to explain its *in vivo* uricosuric effect estimated based on clinical unbound plasma concentrations, suggesting the presence of mechanisms other than competition with UA uptake at the extracellular domain of URAT1 (*cis*-inhibition). In this study, *trans*-inhibition was hypothesized as the mechanism underlying URAT1 inhibition by dotinurad, wherein intracellularly accumulated dotinurad inactivates URAT1. In URAT1-expressing MDCK-II cells and *Xenopus* oocytes, pre-incubation with dotinurad potentiated the inhibitory effect more than co-incubation alone, but this effect was not observed with benzbromarone or probenecid. Under co-incubation, dotinurad inhibited UA uptake in a competitive manner (*cis*-inhibition). When we pre-injected dotinurad directly into oocytes and immediately measured [^{14}C]UA uptake without co-incubation (only *trans*-inhibition), dotinurad noncompetitively inhibited UA uptake. URAT1 is an exchange transporter for UA and monocarboxylates such as nicotinic acid (NA). Pre-injected dotinurad and extracellular UA attenuated and facilitated efflux of [^{3}H]NA, respectively, whereas pre-injection of benzbromarone or probenecid did not affect it, suggesting that dotinurad exhibits *trans*-inhibition by attenuating URAT1-mediated efflux of monocarboxylates, which is a driving

DMD Fast Forward. Published on August 29, 2023 as DOI: 10.1124/dmd.123.001412
This article has not been copyedited and formatted. The final version may differ from this version.

force for UA uptake by URAT1. Accordingly, dotinurad ameliorates URAT1-mediated UA reabsorption by both *cis*- and *trans*-inhibition, explaining its clinically stronger uricosuric effect than that estimated by the *in vitro* IC_{50} value.

DMD Fast Forward. Published on August 29, 2023 as DOI: 10.1124/dmd.123.001412
This article has not been copyedited and formatted. The final version may differ from this version.

Significance Statement

The uricosuric agent dotinurad inhibits uric acid reabsorptive transporter URAT1 with a clinical potency stronger than that estimated from IC_{50} obtained by *in vitro* URAT1 inhibition. This *in vivo-in vitro* discrepancy was explained by the *trans*-inhibition effect of dotinurad on URAT1. *Trans*-inhibition was due to the attenuation of monocarboxylates efflux *via* URAT1, which is a driving force for URAT1-mediated exchange transport of uric acid. Overall, this is the first study to experimentally demonstrate *trans*-inhibition mechanism of URAT1.

DMD Fast Forward. Published on August 29, 2023 as DOI: 10.1124/dmd.123.001412
This article has not been copyedited and formatted. The final version may differ from this version.

Introduction

Hyperuricemia, major cause of gout, is reported to be associated with various diseases, including cardiovascular diseases, chronic kidney disease, fatty liver, and so on; therefore, controlling serum uric acid (UA) levels at less than 6 mg/dL is recommended (Dalbeth et al., 2019). Hyperuricemia is clinically classified as over production type, renal under excretion type, and a mixture of these types based on its pathogenesis causes (Hisatome et al., 2020). As the renal under excretion type is the most common type observed, facilitating urinary excretion of UA using uricosuric agents may be feasible in hyperuricemic patients (Perez-Ruiz et al., 2002). For serum UA lowering therapy (ULT), xanthine oxidase inhibitors that produce UA from purines, and uricosuric agents that promote urinary excretion of UA by inhibiting the renal UA reabsorptive transporter URAT1/*SLC22A12* are available clinically (Jenkins et al., 2022). Probenecid and benzbromarone have been used for a long time as uricosuric agents; their pharmacological target was identified by molecular identification of the URAT1, which takes up UA *via* exchange transport with the efflux of a monocarboxylate such as lactate at the apical membrane of proximal tubular epithelial cells (Enomoto et al., 2002). More recently, lesinurad and dotinurad were approved as uricosuric agents inhibiting URAT1 in some countries; lesinurad is also used in combination with xanthin oxidase inhibitor (Jenkins et al., 2022). The most recently developed agent, dotinurad, may be beneficial owing to its selective inhibition of URAT1 with a negligible effect on other UA transporters such as OAT1/*SLC22A6*, OAT3/*SLC22A8*,

DMD Fast Forward. Published on August 29, 2023 as DOI: 10.1124/dmd.123.001412
This article has not been copyedited and formatted. The final version may differ from this version.

and BCRP/*ABCG2*, which contribute to UA clearance in the kidney and/or small intestine (Taniguchi et al., 2019). As dotinurad lowers serum UA at a dose of 2–4 mg per person (Hosoya et al., 2020) and facilitates urinary excretion of UA (Nakatani et al., 2020), its pharmacological effect is most likely ascribed to inhibition of the URAT1.

The transporter inhibition potential of drugs is usually evaluated by obtaining the half maximal inhibitory concentration (IC_{50}) or the inhibition constant K_i evaluated based on the *in vitro* transport activity measured using the typical substrate for each transporter in the absence and presence of increasing concentrations of the objective inhibitors. However, IC_{50} and/or K_i values obtained *in vitro* may not necessarily be comparable with *in vivo* clinical efficacy. As glomerular filtered UA is taken up by URAT1 to renal proximal tubular epithelial cells from the proximal tubular lumen and dotinurad is expected to interact with UA binding sites at the extracellular domain of URAT1 facing the lumen (*cis*-inhibition), the dotinurad concentration in the lumen, obtained after glomerular filtration, can be used to estimate its inhibition potential (Omura et al., 2020). Plasma unbound drug concentration is then used as a measure of the effective drug concentration in the proximal tubular lumen. In the case of dotinurad, the clinically observed maximum and mean plasma unbound concentration is 10 nM and 2.2 nM, respectively, at a dose of 5 mg/person/day, indicating an almost maximum uricosuric effect of dotinurad (Motoki et al., 2019). In an *in vitro* study, the IC_{50} of dotinurad was obtained as 37.2 nM based on the inhibitory effect of dotinurad on UA uptake by

DMD Fast Forward. Published on August 29, 2023 as DOI: 10.1124/dmd.123.001412
This article has not been copyedited and formatted. The final version may differ from this version.

URAT1-expressing MDCK-II cells (Taniguchi et al., 2019). However, the *in vivo* inhibitory effect of dotinurad was apparently stronger than that estimated from the *in vitro* study. Furthermore, in our pharmacokinetic-pharmacodynamic study, the half maximal effective unbound concentration of dotinurad (EC_{50}) was 3.8 nM, obtained from a plasma concentration of 547 nM, and the unbound fraction was 0.7%, which was smaller than *in vitro* IC_{50} as described above. These observations suggest that the *in vitro* IC_{50} obtained by *cis*-inhibition mechanisms alone may not completely explain the uricosuric effect of dotinurad.

Some drugs such as cyclosporin A exhibit long-lasting inhibition of transporters such as the hepatic uptake transporter OATP1B1, by showing more potent inhibition after pre-incubation in studies *in vitro* (Shitara and Sugiyama, 2017; Izumi et al., 2022). Although the underlying mechanism remains to be fully clarified, modeling analysis and *in vitro* studies combining co- and pre-incubation experiments suggested that this long-lasting effect was attributed to *trans*-inhibition, wherein the intracellularly accumulated drug affects transporter activity (inhibition from inside the cells), in addition to simple *cis*-inhibition (inhibition from outside the cells).

In the present study, to clarify the mechanisms underlying the more potent *in vivo* uricosuric effect of dotinurad than that observed *in vitro* by *cis*-inhibition, we examined whether dotinurad exhibits *trans*-inhibition on URAT1-mediated UA uptake. Further, as dotinurad showed *trans*-inhibition of UA uptake in URAT1-expressing cells, the mechanism underlying *trans*-inhibition by dotinurad was

DMD Fast Forward. Published on August 29, 2023 as DOI: 10.1124/dmd.123.001412
This article has not been copyedited and formatted. The final version may differ from this version.

analyzed.

DMD Fast Forward. Published on August 29, 2023 as DOI: 10.1124/dmd.123.001412
This article has not been copyedited and formatted. The final version may differ from this version.

Materials and Methods

Materials

[8-^{14}C]UA (2.16 TBq/mol) and [^{3}H(G)] 3-pyridinecarboxylic acid (nicotinic acid, 185 TBq/mol) were purchased from Moravek Biochemicals (Brea, CA) and from American Radiolabeled Chemicals (St. Louis, MO), respectively. Dotinurad was obtained from Fuji Yakuhin Co., Ltd. (Saitama, Japan). Lesinurad was obtained from Chemscene (Monmouth Junction, NJ). Probenecid and benzbromarone were from Fujifilm-Wako Pure Chemicals Co. (Osaka, Japan). All other chemicals were commercial products of reagent grade.

Transporter Study by *Xenopus* Oocytes

Xenopus laevis frogs were obtained from Kato-S-Science (Chiba, Japan). UA uptake by URAT1 was examined in *Xenopus laevis* oocytes by culturing them for three days after microinjecting the synthesized complementary RNA (cRNA) for URAT1 as described previously (Iwanaga et al., 2007). Briefly, defolliculated oocytes were injected with 50 nL of water containing 12.5 ng of cRNA of human URAT1 and cultured for three days in modified Barth's solution (MBS, 88 mM NaCl, 1 mM KCl, 2.4 mM $NaHCO_3$, 0.82 mM $MgSO_4$, 0.33 mM $Ca(NO)_3$, 0.41 mM $CaCl_2$, and 10 mM N-(2-hydroxyethyl) piperazine-N′-2-ethanesulfonic acid (HEPES), pH 7.4). To initiate the uptake reaction, oocytes were pre-incubated in ND96 buffer (96 mM NaCl, 2 mM KCl, 1 mM $MgCl_2$, 1.8

DMD Fast Forward. Published on August 29, 2023 as DOI: 10.1124/dmd.123.001412
This article has not been copyedited and formatted. The final version may differ from this version.

mM $CaCl_2$, and 5 mM HEPES, pH 7.4) at 25 °C for 60 min and incubated with Cl^- free uptake buffer (replaced with gluconate of ND96 buffer) containing a mixture of radio-labeled [^{14}C]UA and unlabeled UA at 25 °C for the designated time. Uptake was terminated by washing the oocytes thrice with ice-cold uptake buffer. The uptake (μL/oocyte) was calculated by dividing the uptake amount by the initial concentration of UA in the uptake buffer. As a control, uptake by oocytes injected with the same volume of water was measured using the same procedure. URAT1-mediated uptake was obtained by subtracting the uptake of water-injected oocytes from that of URAT1-overexpressing oocytes.

For the *trans*-inhibitory experiments, 50 nL of each inhibitor was pre-injected into the oocyte and uptake was initiated immediately after pre-injection (within 3 min). For measuring the URAT1-mediated [^{3}H]nicotinic acid (NA) efflux, the efflux was initiated within 3 minutes after injecting 50 nL of 100 μM [^{3}H]NA solution with or without each inhibitor into the oocyte by replacing the incubating buffer with Cl^- free ND96 buffer in the absence or presence of 2 mM UA. The radioactivity in the incubating buffer and oocytes was quantified to estimate the efflux rate of [^{3}H]NA as the percentage of the amount remaining in the oocytes or released into the buffer relative to the total collected radioactivity. Furthermore, to investigate whether inhibition of NA efflux through URAT1 by the *trans*-inhibition affects UA uptake, [^{14}C]UA uptake was measured at the same condition.

DMD Fast Forward. Published on August 29, 2023 as DOI: 10.1124/dmd.123.001412
This article has not been copyedited and formatted. The final version may differ from this version.

Experiments were repeated at least three times (n = 7–17 oocytes for each experiment), and representative results were shown.

Study of Uptake by MDCK-II Cells

Madin–Darby Canine Kidney (MDCK-II)/mock and MDCK-II/URAT1 cells were prepared as described previously (Nakanishi et al., 2013). The cells were cultured in Dulbecco's modified Eagle's medium (Life Technology, Carlsbad, CA) supplemented with 10% (v/v) fetal bovine serum (Life Technology), penicillin, and streptomycin at 37 °C in an atmosphere with 5% CO_2.

Cells were plated in a 12-well plate at a density of 5×10^4 cells/cm^2 and then cultured for two days before the uptake experiments. To initiate the uptake reaction, cells were pre-incubated in transport buffer (136.7 mM NaCl, 0.952 mM $CaCl_2$, 5.36 mM KCl, 0.441 mM KH_2PO_4, 0.812 mM $MgSO_4$, 0.383 mM Na_2HPO_4, 25 mM D-glucose and 25 mM HEPES, pH 7.4) at 37 °C for 60 min and incubated with Cl^- free uptake buffer (Cl^- was replaced with gluconate in transport buffer) containing [^{14}C]UA, at 37 °C for the designated time. Uptake was terminated by washing the cells thrice with fresh ice-cold uptake buffer. A part of the lysate was used for determining total protein amount using a Bradford protein assay with Bio-Rad Protein Assay Kit (Bio-Rad Laboratories, Hercules, CA). The uptake (μL/mg protein) was obtained by dividing the uptake amount by the initial concentration of UA in the uptake buffer and the protein amount in the cells. The URAT1-

DMD Fast Forward. Published on August 29, 2023 as DOI: 10.1124/dmd.123.001412
This article has not been copyedited and formatted. The final version may differ from this version.

mediated uptake rate and inhibitory effect were estimated in the same manner as that in the study on *Xenopus* oocytes using the uptake values of mock cells and the URAT1 cDNA-containing plasmid-transfected cells.

Experiments were repeated at least three times (n = 3–4 for each experiment), and representative results are shown.

Uptake Study by Rat Kidney Slices

Male Wistar rats (150g ~ 170g) were purchased from Japan SLC, Inc. (Hamamatsu, Japan) and acclimatized for more than 3 days before the experiments. The rats were housed with free access to commercial chow and tap water and were maintained on a 12 hours dark/light cycle in an air-controlled room (temperature, 24.0 ± 1 °C; humidity, 55 ± 5%). All animal studies were approved by the Kanazawa University Institutional Animal Care and Use Committee (AP-183955), and the experiments in this study were performed in accordance with the committee. Uptake studies using rat kidney slices were carried out as follows. The slices of whole kidneys were prepared with a micro slicer (Zero 1; Dosaka EM, Kyoto, Japan), and the renal pelvis portion was removed. Prepared slices (300 μm thick) of whole kidneys from male rats were immediately put in ice-cold oxygenated kidney slice (KS) buffer (130 mM NaCl, 4.8 mM KCl, 1.2 mM $CaCl_2$, 1.2 mM $MgSO_4$, 1.2 mM KH_2PO_4 and 25 mM HEPES adjusted to pH 7.4 by NaOH). Three slices from one rat, weighing each

DMD Fast Forward. Published on August 29, 2023 as DOI: 10.1124/dmd.123.001412
This article has not been copyedited and formatted. The final version may differ from this version.

slice 2 to 10 mg, were randomly selected and then preincubated in a 12-well plate with 1 mL of oxygenated KS buffer in each well at 37 °C for 5 min. After pre-incubation, the kidney slices were put into KS buffer containing dotinurad (100 nM) with or without 1 mM probenecid to initiate the uptake reaction. The uptake reactions were carried out at 37 °C for an appropriate time, and then each slice was rapidly removed from the KS buffer, washed twice with 2 mL of ice-cold KS buffer, blotted on filter paper to remove adherent buffer solution and weighed. For the measurement of dotinurad, the slices were homogenized in 70% methanol, and centrifuged at 15,000 × g for 15 min at 4 °C to obtain the supernatant to analyze with LC-MS/MS system. Concentration of dotinurad was measured by an LCMS-8050 triple quadrupole LC-MS/MS (Shimadzu, Kyoto, Japan) coupled to an LC-30A system (Shimadzu). The mobile phase was composed of a mixture of 5 mM ammonium acetate (A phase) and methanol (B phase) at the flow rate of 0.28 mL/min. Chromatography was performed on a Inertsil ODS-3 (3 μm, 2.1 × 150 mm, GL. Science, Tokyo, Japan) at 40 °C with an injection volume of 10 μL. The mobile phase isocratic elution maintained at 80% solvent B for 8 min. The detected mass numbers and collision energy (CE) were 355.95→159.90 and CE −22 V, respectively. Labsolutions software (version 5.89, Shimadzu) was used for data manipulation. The detection limit of dotinurad was 1 nM. Uptake amount was shown as tissue to medium ratio obtained by dividing uptake amount by medium concentration of dotinurad and shown as μL/mg kidney.

DMD Fast Forward. Published on August 29, 2023 as DOI: 10.1124/dmd.123.001412
This article has not been copyedited and formatted. The final version may differ from this version.

Analytical Methods

[^{14}C]UA and [^{3}H]NA were measured using a liquid scintillation counter (LSC8000; Aloka, Tokyo, Japan) after adding liquid scintillation cocktail (Clear-sol I; Nacalai Tesque, Kyoto, Japan) to each sample. The inhibitory effects of drugs on UA uptake were shown as percentage of the control and kinetic parameters for the inhibitory effect were estimated using a non-linear least-squares regression analysis in KaleidaGraph 4.0 (Synergy Software, Reading, PA), according to the following equation (1):

$$\% \text{ of control} = 100 \times IC_{50}/(IC_{50} + \mathrm{I}) \quad \cdots \quad (1)$$

where, IC_{50} and I are the half maximum inhibitory concentration and concentration of the inhibitor used, respectively. To evaluate the uptake kinetic parameters, the rates were fitted to the following equation (2):

$$v = (V_{max} \times S)/(K_m + S) \quad \cdots \quad (2)$$

where v, S, K_m, and V_{max} are the uptake rate of the substrate (pmol per indicated time per oocyte), the substrate (UA) concentration in the uptake medium (μM), the Michaelis–Menten constant (μM), and the maximal uptake rate (pmol per indicated time per oocyte), respectively. To evaluate the inhibitory constant (K_i), K_i for competitive or noncompetitive-type inhibitions was fitted to the following equations (3) and (4), respectively:

$$v = (V_{max} \times S)/(K_m \times(1 + I/K_i) + S) \quad \cdots \quad (3)$$

DMD Fast Forward. Published on August 29, 2023 as DOI: 10.1124/dmd.123.001412
This article has not been copyedited and formatted. The final version may differ from this version.

$$v = (V_{max} \times S)/((K_m + S) \times (1 + I/K_i)) \quad \cdots \quad (4)$$

where K_i is the inhibition constant.

All data are presented as the mean ± SD. Kinetic parameters obtained using the nonlinear least-square regression analysis are shown as the mean ± SEM, obtained using the software KaleidaGraph ver. 4.0. Statistical significance was examined using the Student's *t*-test and Dunnett's test ($p < 0.05$).

DMD Fast Forward. Published on August 29, 2023 as DOI: 10.1124/dmd.123.001412
This article has not been copyedited and formatted. The final version may differ from this version.

Results

Effect of Pre-incubation on the Inhibition Potencies of Uricosuric Agents for UA Uptake by URAT1 in *Xenopus* Oocytes and MDCK-II Cells Expressing URAT1

The concentration-dependent effect of uricosuric agents on UA uptake (10 μM [^{14}C]UA) by URAT1-expressing oocytes for 20 min was studied with and without 60 min of pre-incubation with each uricosuric agent (Fig. 1A-D). The half maximal inhibitory concentrations (IC_{50}) of dotinurad, lesinurad, benzbromarone, and probenecid were 24.5, 88,200, 329, and 326,000 nM, respectively, when these uricosuric agents were added only during uptake measurement (Co-incubation alone). When these agents were pre-incubated for 60 min and subsequently incubated for 20 min with [^{14}C]UA (Pre- and Co-incubations), their IC_{50} values were 11.0, 52,700, 355, and 293,000 nM, respectively. These IC_{50} values at each condition are summarized in Table 1. The IC_{50} ratios, (Pre- and Co-incubation)/(Co-incubation alone), were 0.45, 0.60, 1.1, and 0.9 for dotinurad, lesinurad, benzbromarone, and probenecid, respectively. Ratios less than unity observed for dotinurad and lesinurad suggest that their inhibition strength was potentiated by pre-incubation, while such a potentiation by pre-incubation was not observed for benzbromarone and probenecid. These results suggest that dotinurad and lesinurad inhibit URAT1 in a pre-incubation-dependent manner.

The same experiments were conducted in MDCK-II cells expressing URAT1 (MDCK-II/URAT1), to confirm the observed difference in pre-incubation effects among uricosuric agents in *Xenopus*

DMD Fast Forward. Published on August 29, 2023 as DOI: 10.1124/dmd.123.001412
This article has not been copyedited and formatted. The final version may differ from this version.

oocytes (Fig. 1E-H). Each agent reduced the URAT1-mediated UA uptake in a concentration-dependent manner with and without pre-incubation. However, similar to the results obtained in *Xenopus* oocytes, dotinurad and lesinurad exhibited smaller IC_{50} values at the condition of pre- and co-incubation compared with those in co-incubation alone showing IC_{50} ratios of 0.42 and 0.34, respectively. However, the IC_{50} ratios of benzbromarone (1.19) and probenecid (1.43) were comparable between the conditions with and without pre-incubation (Table 1). Accordingly, dotinurad and lesinurad were showed to exhibit pre-incubation dependent inhibitory effects on URAT1.

Trans-inhibition Effect of Uricosuric Agents on UA Uptake by URAT1 in _Xenopus_ Oocytes Expressing URAT1

Although the mechanism of pre-incubation effects observed for dotinurad and lesinurad is unclear, we hypothesized that such uricosuric agents inhibit URAT1-mediated UA uptake from the intracellular side of URAT1. In this study, we defined the inhibition mode of UA uptake from the intracellular side as *trans*-inhibition effect. Inhibition of UA uptake from the extracellular side of URAT1 is thus referred as *cis*-inhibition. Technically, the pre-incubation effect could be affected by the membrane permeability of the agents; further, the cell surface adhered agents may not be completely cleared by washing the cells before uptake measurement. In case of the latter, it is

DMD Fast Forward. Published on August 29, 2023 as DOI: 10.1124/dmd.123.001412
This article has not been copyedited and formatted. The final version may differ from this version.

difficult to differentiate the effect of adhered agents to cell surface from the true *trans*-inhibition effect. Accordingly, the following *trans*-inhibition study was conducted by pre-injecting each agent directly into oocytes just prior to the uptake measurement.

The *trans*-inhibitory effect of uricosuric agents on UA uptake was measured immediately after pre-injecting 50 nL of each agent into URAT1-expressing *Xenopus* oocytes. URAT1-mediated UA uptake for 20 min was decreased significantly by pre-injecting dotinurad (50 μM) and lesinurad (5 mM) (Fig. 2A). In contrast, pre-injected benzbromarone (250 μM) or probenecid (2 mM) did not affect UA uptake. Here, the used concentration of each agent was set much higher than the IC_{50} of co-incubation shown in Table 1, as pre-injected drug (50 nL) is diluted by intracellular fluid (approximately 20-times) (Iwanaga et al., 2007). In the case of probenecid, the preinjected concentration may not be high enough owing to limited solubility in the injected solvent. To confirm the observed *trans*-inhibition effect, dependence on the pre-injected drug concentration was examined. The results are shown in Figure 2B. Dotinurad (1, 2, 5, 10, and 50 μM, injected drug concentrations shown by open circles) and lesinurad (1 and 5 mM shown by closed triangles) exhibited a concentration-dependent decrease in UA uptake activity. In contrast, the effect of benzbromarone (50 and 200 μM, shown by closed circles) and probenecid (0.2 and 2 mM shown by open triangles) on UA uptake was comparable at those concentrations and was mostly equal to that of the control (open square). These results support that dotinurad and lesinurad specifically affect

DMD Fast Forward. Published on August 29, 2023 as DOI: 10.1124/dmd.123.001412
This article has not been copyedited and formatted. The final version may differ from this version.

URAT1 from inside (*trans*-inhibition), whereas benzbromarone and probenecid do not, showing differential interaction with URAT1 among uricosuric agents.

Cis- and _trans_-Inhibition Kinetics of Dotinurad on URAT1-mediated UA Uptake in _Xenopus_ Oocytes Expressing URAT1

Dotinurad is one of the most potent URAT1 inhibitors with the lowest IC_{50} value (*cis*-inhibition), and exhibits inhibition potential from both outside (*cis*-inhibition) and inside (*trans*-inhibition) cells. The *cis*- and *trans*-inhibition modes of dotinurad were kinetically analyzed by changing concentrations of UA and dotinurad. The results are shown in Figure 3. Figures 3A, B and C show the Eadie-Hofstee plot for the *cis*-inhibition of URAT1-mediated UA uptake by dotinurad at 20 (A), 40 (B), and 80 nM (C). At all concentrations of dotinurad, the x-intercept values were comparable both in the absence and presence of dotinurad, while the slope of the regression line declined in the presence of dotinurad compared with that in the absence of dotinurad. Further, the obtained kinetic parameters obtained are shown in Table 2. Compared with the differences in V_{max} values among the different concentrations of dotinurad, the change in K_m values with dotinurad was more evident. Accordingly, dotinurad most likely inhibits URAT1-mediated UA uptake in a competitive manner. Simultaneous least squares analysis of the plots considering competitive inhibition kinetics resulted a K_i value of 27.2 ± 1.6 nM for dotinurad, which was close to the K_i values obtained at each dotinurad

DMD Fast Forward. Published on August 29, 2023 as DOI: 10.1124/dmd.123.001412
This article has not been copyedited and formatted. The final version may differ from this version.

concentration (Table 2).

Figure 3D shows the Eadie-Hofstee plot for the *trans*-inhibition of URAT1-mediated UA uptake by pre-injected dotinurad at 0 and 50 μM. The x-intercept values exhibited a significant difference between the presence and absence of dotinurad, while the slopes were comparable. When kinetic parameters were obtained as shown in Table 2, the apparent K_m values were comparable (93.3 and 113 μM), while the apparent *Vmax* value decreased by more than 2-times from 22.9 to 9.93 pmol/20 min/oocyte in the absence and presence of dotinurad pre-injection, respectively. Accordingly, *trans*-inhibition by dotinurad was explained by noncompetitive inhibition kinetics with a K_i value of 32.5 ± 0.941 μM based on the injected dotinurad concentrations. Considering a 20-fold dilution of pre-injected dotinurad solution in the oocytes, the final concentration would be approximately 1.6 μM (Iwanaga et al., 2007). These results demonstrated that dotinurad competes for the same binding site of UA on the extracellular domain of URAT1. In contrast, dotinurad interacts allosterically on URAT1 inside the cells.

Mechanism of *Trans*-inhibition of URAT1 by Dotinurad in URAT1-expressing *Xenopus* Oocytes

The mechanism of *trans*-inhibition by dotinurad was further studied focusing on the interaction with the driving force of URAT1-mediated UA uptake. URAT1 is known as an exchange transporter for

DMD Fast Forward. Published on August 29, 2023 as DOI: 10.1124/dmd.123.001412
This article has not been copyedited and formatted. The final version may differ from this version.

inward UA uptake and outward efflux of monocarboxylates like lactic acid and nicotinic acid (Enomoto et al., 2002). As we have previously reported that preloading nicotinic acid into URAT1-expressing oocytes significantly facilitated UA uptake (Lu et al., 2013), we examined the *trans*-inhibition effect of dotinurad and other uricosuric agents on NA efflux from *Xenopus* oocytes after pre-injecting a 50 nL aliquot of [^{3}H]NA (100 μM). Figure 4A shows the [^{3}H]NA amount remaining in the oocytes at 120 min after pre-injecting both [^{3}H]NA and each uricosuric agent into the oocytes simultaneously. To evaluate the URAT1-mediated exchange transport of UA with NA, the remaining amount of [^{3}H]NA was compared between the presence and absence of extracellular UA (2 mM). In water-injected oocytes which did not express URAT1, a comparable amount of [^{3}H]NA remained in the oocytes in the absence (62%) and presence (65%) of extracellular UA and the remaining amount was higher than that in *Xenopus* oocytes expressing URAT1. In control oocytes expressing URAT1 without pre-injecting any uricosuric agent, the remaining amount of [^{3}H]NA was significantly lower than that of water-injected oocytes at 19% and 36% in the presence and absence of extracellular UA, respectively. Such a low remaining amount in the presence of extracellular UA is explained by URAT1-mediated exchange efflux of [^{3}H]NA with UA uptake; therefore, this method was considered suitable for evaluating the NA efflux *via* UART1. When dotinurad was pre-injected, the remaining amount of [^{3}H]NA was comparable between the presence (34%) and absence (36%) of extracellular UA. This result suggested that dotinurad inhibited the URAT1-mediated exchange

DMD Fast Forward. Published on August 29, 2023 as DOI: 10.1124/dmd.123.001412
This article has not been copyedited and formatted. The final version may differ from this version.

efflux of [^{3}H]NA with extracellular UA. A similar result was observed with the pre-injection of lesinurad. In contrast, in oocytes pre-injected with benzbromarone or probenecid, the remaining amount of [^{3}H]NA in the presence of extracellular UA was less than that in the absence of extracellular UA. Accordingly, these two uricosuric agents are unlikely to affect the UA-dependent efflux of [^{3}H]NA. Figure 4B shows the same results as those in Fig. 4A, but with magnified exchange transport with extracellular UA, by showing the remaining amount of [^{3}H]NA in the absence of extracellular UA as 100%. Thus, pre-injection of dotinurad and lesinurad clearly abolished URAT1-mediated exchange efflux of [^{3}H]NA with UA uptake, but this was not observed with benzbromarone or probenecid.

To confirm that the NA efflux is coupled with UA uptake, [^{14}C]UA uptake was measured under the same condition. Figure 4C shows the uptake of [^{14}C]UA (2 mM, 30 min) by *Xenopus* oocytes pre-injected with 100 μM unlabeled NA and each uricosuric agent. Firstly, in control oocytes expressing URAT1 without uricosuric agents, [^{14}C]UA uptake was significantly higher than that in water-injected oocytes that do not express URAT1. Uptake of [^{14}C]UA was decreased by pre-injecting dotinurad and lesinurad, whereas pre-injecting benzbromarone or probenecid had no such effect. Accordingly, the results observed in Fig. 4A and 4B were confirmed to be due to the exchange transport of UA and NA mediated by URAT1. These results support that dotinurad and lesinurad decrease the efflux of [^{3}H]NA, which is dependent on URAT1 and extracellular UA, whereas

DMD Fast Forward. Published on August 29, 2023 as DOI: 10.1124/dmd.123.001412
This article has not been copyedited and formatted. The final version may differ from this version.

benzbromarone and probenecid do not affect it. All these results suggest that the *trans*-inhibition mechanism of dotinurad and lesinurad is an inhibition of the efflux of monocarboxylic acid that is exchanged with the influx of UA *via* URAT1.

Uptake of Dotinurad by Rat Kidney Slices

The mechanism of *trans*-inhibition by dotinurad was further evaluated measuring accumulation of dotinurad in the kidney tissues. Uptake of dotinurad (100 nM) by rat kidney slices in the presence or absence of probenecid (1 mM) as an organic anion transporter inhibitor. Figure 5 shows time course for the uptake dotinurad over 60 min. Dotinurad uptake was increased with time and was significantly decreased in the presence of 1 mM probenecid (Fig. 5). The result suggests that dotinurad is a substrate of OATs.

DMD Fast Forward. Published on August 29, 2023 as DOI: 10.1124/dmd.123.001412
This article has not been copyedited and formatted. The final version may differ from this version.

Discussion

The present study examined the *trans*-inhibition potential of the uricosuric agent dotinurad for the UA reabsorptive transporter URAT1 to clarify the mechanism of apparent discrepancy in the uricosuric effect of dotinurad between the *in vitro* observed IC_{50} on URAT1 (Taniguchi et al., 2019) and the *in vivo* estimated uricosuric effect obtained using pharmacokinetic-pharmacodynamic simulation studies and the observed plasma unbound concentrations of dotinurad (Motoki et al., 2019).

URAT1 is an exchange transporter that acts by taking up UA and is energized by the efflux of monocarboxylates like lactate and nicotinate (Enomoto et al., 2002; Lu et al., 2013). Further, clinically used drugs such as pyrazine carboxylic acid, a metabolite of the antituberculosis agent pyrazinamide, low concentrations of salicylic acid, and some angiotensin II receptor blockers activate the uptake of UA from the inside the cells showing a *trans*-stimulation effect (Iwanaga et al., 2007; Li et al., 2008; Nakanishi et al., 2013). In contrast, URAT1 is *cis*-inhibited by drugs such as losartan, indomethacin, and high concentrations of salicylate as well as the clinically available uricosuric agents used in the present study (Enomoto et al., 2002; Iwanaga et al., 2007; Li et al., 2008; Shin et al., 2011; Nakanishi et al., 2013). Accordingly, as URAT1 is prone to be affected by variable drugs, we hypothesized that URAT1 can be inhibited by intracellularly accumulated dotinurad, showing *trans*-inhibition.

DMD Fast Forward. Published on August 29, 2023 as DOI: 10.1124/dmd.123.001412
This article has not been copyedited and formatted. The final version may differ from this version.

First, we examined the effect of dotinurad pre-incubation on the uptake of [^{14}C]UA by both URAT1-expressing oocytes and MDCK-II cells. Compared with the IC_{50} of dotinurad without pre-incubation, the IC_{50} was decreased from 25 to 11 nM in *Xenopus* oocytes and from 80 to 33 nM in MDCK-II cells when the cells were preincubated with dotinurad for 60 min (Fig. 1 and Table 1). Lesinurad also exhibited a pre-incubation effect similar to that of dotinurad. However, the conventional uricosuric agents, benzbromarone and probenecid, did not exhibit such a decrease in IC_{50} by pre-incubation. Accordingly, the pre-incubation effect on URAT1 varies with the uricosuric agent used and both dotinurad and lesinurad exhibit *trans*-inhibition of URAT1; however, the molecular structure of the agents responsible for *trans*-inhibition is not clear.

One possible mechanism of the pre-incubation effect is that drugs taken up by cells inhibit URAT1 from inside the cells, thus being affected by the intracellular drug concentrations. When URAT1-expressing cells were pre-incubated with uricosuric agents in the uptake medium, the intracellularly accumulated amount of drugs gradually increased with time. Accordingly, it is difficult to control the intracellular effective drug concentration using the pre-incubation method; therefore, the pre-incubation method may not be adequate to kinetically examine whether the drug shows a *trans*-inhibition effect. As dotinurad and lesinurad were suggested to exhibit *trans*-inhibition in the pre-incubation study, we took advantage of experimental methods using *Xenopus* oocytes to evaluate *trans*-inhibition by directly injecting uricosuric agents into each oocyte in the following experiments.

DMD Fast Forward. Published on August 29, 2023 as DOI: 10.1124/dmd.123.001412
This article has not been copyedited and formatted. The final version may differ from this version.

The results showed that pre-injection of dotinurad and lesinurad decreased the [^{14}C]UA uptake significantly, while such an effect was not observed with benzbromarone or probenecid (Fig. 2), confirming that the observed *trans*-inhibition effect is compound-specific as observed using the pre-incubation method (Fig. 1). Furthermore, the observed *trans*-inhibition effect was dependent on the injected drug concentrations, suggesting that the observation is a specific phenomenon but not an experimental artifact. However, the decreased URAT1 activity by pre-incubation may include additional mechanisms such as altered expression of URAT1 protein, since clinically the exposure time of URAT1 with dotinurad is much longer during dotinurad treatment. Moreover, a kinetic study of the inhibitory effect of dotinurad showed competitive and noncompetitive type inhibition for *cis*-inhibition and *trans*-inhibition, respectively (Fig. 3). Accordingly, dotinurad is likely to share the same binding site with UA on the extracellular domain of URAT1; however, the *trans*-inhibition site of dotinurad is not the same as the binding site of UA on URAT1 uptake site. The observed noncompetitive inhibition kinetics are reasonable, as dotinurad was directly injected into intracellular space and is unable to compete with UA binding site on the extracellular domain of URAT1.

URAT1 is well known as an exchange transporter for extracellular UA and intracellular monocarboxylates such as nicotinic acid; intracellular monocarboxylates activate URAT1-mediated UA uptake by counterflow from the inside to outside the cells (Enomoto et al., 2002). This activation

DMD Fast Forward. Published on August 29, 2023 as DOI: 10.1124/dmd.123.001412
This article has not been copyedited and formatted. The final version may differ from this version.

can be called a *trans*-stimulation effect and is clearly observed in our *Xenopus* oocytes study, as we have already reported that UA uptake by URAT1 is accelerated by intracellular monocarboxylates, specifically nicotinic acid (Lu et al., 2013). Accordingly, intracellular monocarboxylates should have a binding site in the cytosolic region of URAT1. We then hypothesized that dotinurad may compete for the flux of monocarboxylates from the intracellular domain of URAT1 and thus examined efflux of [^{3}H]NA exchanged with extracellular UA *via* URAT1 (Lu et al., 2013). Extracellular UA-dependent efflux of [^{3}H]NA was clearly observed, and was attenuated by pre-injection of dotinurad and lesinurad, while benzbromarone or probenecid had no effect (Fig. 4A, B). Along with the decrease in NA efflux, [^{14}C]UA uptake was decreased by pre-injection of dotinurad and lesinurad (Fig. 4C). These results confirmed that NA efflux and UA uptake are directly coupled and that dotinurad and lesinurad interact with the intracellular site of URAT1 responsible for the intracellular monocarboxylate transport, showing noncompetitive-type inhibition kinetics for apparent UA uptake. As dotinurad is highly permeable because its bioavailability is high (90%) and is mostly excreted into urine, dotinurad can be accumulated in renal tubular epithelial cells clinically (Omura et al., 2020). Accordingly, dotinurad accumulated in renal tubular epithelial cells exhibits *trans*-inhibition from the intracellular side as well as *cis*-inhibition from the tubular lumen side. In addition, dotinurad was taken up by kidney slices in a probenecid-sensitive manner (Fig. 5), which suggests that dotinurad is actively taken up by the kidney from blood and secreted into urine, leading

DMD Fast Forward. Published on August 29, 2023 as DOI: 10.1124/dmd.123.001412
This article has not been copyedited and formatted. The final version may differ from this version.

to higher luminal concentration than glomerular filtrate. Accordingly, such a tubular secretion of dotinurad may also explain its more potent URAT1 inhibition than expected from plasma unbound concentration. Clinically, the inhibition modes of dotinurad on URAT1 are considered at the pre-incubation condition; therefore, *trans*-inhibition as well as *cis*-inhibition should both be activated in *vivo*, resulting in the more potent uricosuric effect in *in vivo* compared with that in *in vitro*, which reflects only *cis*-inhibition. However, further studies are needed to show the contribution of the *trans*-inhibition effect as a mechanism to explain the apparent discrepancy of the uricosuric effect of dotinurad between the *in vitro* and *in vivo* settings. However, the results obtained in the present study strongly demonstrated that *trans*-inhibition of URAT1 by dotinurad contributes to clinically stronger URAT1-inhibitory potential than that estimated from *in vitro cis*-inhibition potential. For lesinurad, although there is no report on kidney tissue accumulation, it was reported in the assessment report of Zurampic, a marketed product of lesinurad, that lesinurad is highly permeable, excreted into urine efficiently and is a substrate of organic anion transporter OATs (https://www.ema.europa.eu/en/documents/assessment-report/zurampic-epar-public-assessment-report_en.pdf). These characteristics of lesinurad suggest that it is accumulated in kidney and exhibit *trans*-inhibition of URAT1 in the similar manner with dotinurad.

Drug-drug interactions (DDI) on transporters have been known to cause clinical problems due to altered exposure of the target drugs by co-administered perpetrating drugs. In some transporters such

DMD Fast Forward. Published on August 29, 2023 as DOI: 10.1124/dmd.123.001412
This article has not been copyedited and formatted. The final version may differ from this version.

as hepatic OATP1B1, pre-incubation of perpetrating drugs such as cyclosporin A and everolimus with the transporter-expressing cells or cultured hepatocytes potentiates their inhibitory effect, suggesting more significant clinical problems than those estimated from *in vitro* DDI (Shitara and Sugiyama, 2017; Farasyn et al., 2021). Such a pre-incubation dependent DDI is explained by *trans*-inhibition, caused by perpetrating drugs accumulated in the cells as indicated by studying the modeling analysis (Izumi et al., 2022). In the case of mTOR inhibitors such as everolimus, their pharmacological effect to inhibit phosphorylation of OATP1Bs was excluded as a pre-incubation effect and certain interaction of those drugs on the intracellular side of the transporters was proposed (Farasyn et al., 2019). In the case of Na^+/taurocholate cotransporting polypeptide (NTCP), taurolithocholate exhibits a pre-incubation effect on NTCP most likely due to binding to the intracellular domain of NTCP (Lowjaga et al., 2021). Other possible mechanisms for the pre-incubation effect include internalization of transporter proteins from the membrane to cytosolic domain and decreased protein expression. Although these studies have demonstrated that transporters are subject to pre-incubation effects by various drugs, the mechanisms are not directly clarified. Accordingly, the present study provides the first experimental demonstration of the mechanism underlying the preincubation effect of URAT1 inhibitors by affecting the flux of monocarboxylic acids that provide a driving force for UA uptake by URAT1.

In conclusion, we demonstrated that dotinurad facilitates the urinary excretion of UA by decreasing

DMD Fast Forward. Published on August 29, 2023 as DOI: 10.1124/dmd.123.001412
This article has not been copyedited and formatted. The final version may differ from this version.

URAT1 activity *via trans*-inhibition as well as *cis*-inhibition. *Trans*-inhibition was suggested to occur due to inhibition of the coupled exchange transport of monocarboxylic acid with UA *via* URAT1. Overall, the t*rans*-inhibitory effect of URAT1 is a novel mechanism of drug-induced changes in serum UA levels and may explain the apparently stronger effect observed clinically than that indicated by the *in vitro* IC_{50} values of dotinurad.

DMD Fast Forward. Published on August 29, 2023 as DOI: 10.1124/dmd.123.001412
This article has not been copyedited and formatted. The final version may differ from this version.

Data Availability Statement

All the data supporting the findings of this study are contained within the paper.

Authorship Contributions

Participated in research design: Tamai, Fujita.

Conducted experiments: Fujita, Zhu

Performed data analysis: Fujita, Zhu, Arakawa

Wrote or contributed to the writing of the manuscript: Fujita, Zhu, Shirasaka, Tamai

References

Dalbeth N, Choi HK, Joosten LAB, Khanna PP, Matsuo H, Perez-Ruiz F, and Stamp LK (2019) Gout. *Nature Rev Dis primers* **5:**69.

Enomoto A, Kimura H, Chairoungdua A, Shigeta Y, Jutabha P, Cha SH, Hosoyamada M, Takeda M, Sekine T, Igarashi T, Matsuo H, Kikuchi Y, Oda T, Ichida K, Hosoya T, Shimokata K, Niwa T, Kanai Y, and Endou H (2002) Molecular identification of a renal urate anion exchanger that regulates blood urate levels. *Nature* **417:**447-452.

Farasyn T, Crowe A, Hatley O, Neuhoff S, Alam K, Kanyo J, Lam TT, Ding K, and Yue W (2019) Preincubation with everolimus and sirolimus reduces organic anion-transporting polypeptide (OATP)1B1- and 1B3-mediated transport independently of mTOR kinase inhibition: Implication inassessing OATP1B1- and OATP1B3-mediated drug-drug interactions. *J Pharm Sci* **108:**3443-3456.

Farasyn T, Pahwa S, Xu C, and Yue W (2021) Pre-incubation with OATP1B1 and OATP1B3 inhibitors potentiates inhibitory effects in physiologically relevant sandwich-cultured primary human hepatocytes. *Eu J Pharm Sci* **165:**105951.

Hisatome I, Ichida K, Mineo I, Ohtahara A, Ogino K, Kuwabara M, Ishizaka N, Uchida S, Kurajoh M, Kohagura K, Sato Y, Taniguchi A, Tsuchihashi T, Terai C, Nakamura T, Hamaguchi T, Hamada T, Fujimori S, Masuda I, Moriwaki Y, and Yamamoto T (2020) Japanese Society of Gout and

DMD Fast Forward. Published on August 29, 2023 as DOI: 10.1124/dmd.123.001412
This article has not been copyedited and formatted. The final version may differ from this version.

Uric and Nucleic Acids 2019 Guidelines for Management of Hyperuricemia and Gout 3rd edition. *Gout Uric & Nucleic Acids* **44:**sp-1-sp-40.

Hosoya T, Fushimi M, Okui D, Sasaki T, and Ohashi T (2020) Open-label study of long-term administration of dotinurad in Japanese hyperuricemic patients with or without gout. *Clin Exp Nephrol* **24:**80-91.

Iwanaga T, Sato M, Maeda T, Ogihara T, and Tamai I (2007) Concentration-dependent mode of interaction of angiotensin II receptor blockers with uric acid transporter. *J Pharmacol Exp Ther* **320:**211-217.

Izumi S, Nozaki Y, Lee W, and Sugiyama Y (2022) Experimental and modeling evidence supporting the trans-inhibition mechanism for preincubation time-dependent, long-lasting inhibition of organic anion transporting polypeptide 1B1 by cyclosporine A. *Drug Metab Dispos* **50:**541-551.

Jenkins C, Hwang JH, Kopp JB, Winkler CA, and Cho SK (2022) Review of urate-lowering therapeutics: From the past to the future. *Front Pharmacol* **13:**925219.

Li Y, Sato M, Yanagisawa Y, Mamada H, Fukushi A, Mikami K, Shirasaka Y, Tamai I. (2008) Effects of angiotensin II receptor blockers on renal handling of uric acid in rats. *Drug Metab Pharmacokinet* **23**: 263-270.

Lowjaga K, Kirstgen M, Müller SF, Goldmann N, Lehmann F, Glebe D, and Geyer J (2021) Long-term trans-inhibition of the hepatitis B and D virus receptor NTCP by taurolithocholic acid. *Am J*

Physiol **320:**G66-G80.

Lu Y, Nakanishi T, and Tamai I (2013) Functional cooperation of SMCTs and URAT1 for renal reabsorption transport of urate. *Drug Metab Pharmacokinet* **28:**153-158.

Motoki K, Igarashi T, Omura K, Nakatani H, Iwanaga T, Tamai I, and Ohashi T (2019) Pharmacokinetic/pharmacodynamic modeling and simulation of dotinurad, a novel uricosuric agent, in healthy volunteers. *Pharmacol Res Perspec* **7:**e00533.

Nakanishi T, Ohya K, Shimada S, Anzai N, and Tamai I (2013) Functional cooperation of URAT1 (SLC22A12) and URATv1 (SLC2A9) in renal reabsorption of urate. *Nephrol Dial Transplant* **28:**603-611.

Nakatani H, Fushimi M, Sasaki T, Okui D, and Ohashi T (2020) Clinical pharmacological study of dotinurad administered to male and female elderly or young subjects. *Clin Exp Nephrol* **24:**8-16.

Omura K, Miyata K, Kobashi S, Ito A, Fushimi M, Uda J, Sasaki T, Iwanaga T, and Ohashi T (2020) Ideal pharmacokinetic profile of dotinurad as a selective urate reabsorption inhibitor. *Drug Metab Pharmacokinet* **35:**313-320.

Perez-Ruiz F, Calabozo M, Erauskin GG, Ruibal A, and Herrero-Beites AM (2002) Renal underexcretion of uric acid is present in patients with apparent high urinary uric acid output. *Arthritis Rheum* **47:**610-613.

Shin HJ, Takeda M, Enomoto A, Fujimura M, Miyazaki H, Anzai N, and Endou H (2011) Interactions of

urate transporter URAT1 in human kidney with uricosuric drugs. *Nephrology* **16:**156-162.

Shitara Y and Sugiyama Y (2017) Preincubation-dependent and long-lasting inhibition of organic anion transporting polypeptide (OATP) and its impact on drug-drug interactions. *Pharmacol Ther* **177:**67-80.

Taniguchi T, Ashizawa N, Matsumoto K, Saito R, Motoki K, Sakai M, Chikamatsu N, Hagihara C, Hashiba M, and Iwanaga T (2019) Pharmacological evaluation of dotinurad, a selective urate reabsorption inhibitor. *J Pharmacol Exp Ther* **371:**162-170.

DMD Fast Forward. Published on August 29, 2023 as DOI: 10.1124/dmd.123.001412
This article has not been copyedited and formatted. The final version may differ from this version.

Footnotes

This study was supported by Grant-in-Aid for Scientific Research (B) [21H02641] (IT) from the Japan Society for the Promotion of Science (JSPS).

No author has an actual or perceived conflict of interest with the contents of this article.

Reprint requests:

Ikumi Tamai, Ph.D.,

Faculty of Pharmaceutical Sciences, Institute of Medical, Pharmaceutical and Health Sciences, Kanazawa University

Kakuma-machi, Kanazawa 920-1192, Japan.

Tel: +81-76-234-4479; Fax: +81-76-264-6284

Mail: tamai@p.kanazawa-u.ac.jp

DMD Fast Forward. Published on August 29, 2023 as DOI: 10.1124/dmd.123.001412
This article has not been copyedited and formatted. The final version may differ from this version.

Figure Legends

Figure 1. Pre-incubation effect of uricosuric agents on URAT1-mediated uric acid uptake in *Xenopus* oocytes (A-D) or MDCK-II cells (E-H).

Experiments involving co-incubation (open circles, solid line) and pre-incubation + co-incubation (closed squares, dashed line) of various inhibitors were performed. Cells were pre-incubated with and without dotinurad (A, E), lesinurad (B, F), benzbromarone (C, G), or probenecid (D, H) for 60 min and uptake studies were carried out replacing the incubation medium with the uptake buffer containing 10 μM [^{14}C]UA and respective inhibitors. URAT1-mediated uptake was determined by subtracting the uptake by water-injected oocytes from that by URAT1-expressing oocytes (A-D) or the uptake by MDCK-II/mock cells from that by MDCK-II/URAT1 (E-H). The values obtained were divided by the control value in each assay and are shown as percentages of uptake in the absence of an inhibitor.

Each point represents the mean ± SD. *: Significantly different from the co-incubation group by Student's *t*-test ($p < 0.05$).

Figure 2. *Trans*-inhibition effect of uricosuric agents on URAT1-mediated UA uptake in *Xenopus* oocytes.

(A) URAT1-mediated uptake of [^{14}C]UA (10 μM) by oocytes was measured after pre-injecting 50 nL of water (control) or uricosuric agents for 60 min. Injected concentrations of each uricosuric agent

DMD Fast Forward. Published on August 29, 2023 as DOI: 10.1124/dmd.123.001412
This article has not been copyedited and formatted. The final version may differ from this version.

were dotinurad (50 μM), lesinurad (5 mM), benzbromarone (250 μM) and probenecid (2 mM). (B) URAT1-mediated uptake of [^{14}C]UA (10 μM) by oocytes was measured after preloading 50 nL of water (open square), dotinurad (1, 2, 5, 10, 50 μM, open circles), lesinurad (1 and 5 mM, closed triangles), benzbromarone (50 and 250 μM, closed circles), and probenecid (0.2 and 2 mM, open triangles) for 20 min.

Each point represents the mean ± SD. *: Significantly different from the control (A) or uptake in the presence of the lowest concentrations of each uricosuric agent (B) using Dunnett's test ($p < 0.05$).

Figure 3. Eadie-Hofstee plots of the *cis*-inhibitory (A-C) and *trans*-inhibitory (D) effect of dotinurad on uptake of UA by URAT1.

(A-C) URAT1-mediated uptake of [^{14}C]UA (10, 30, 50, 100, 300 μM) by oocytes was measured in the absence (A-C, open circles) or presence of 20 nM (A, closed triangles), 40 nM (B, closed squares), 80 nM (C, closed diamond) dotinurad for 60 min. (D) URAT1-mediated uptake of [^{14}C]UA (10, 30, 50, 70, 100, 300, 500, 700, and 1000 μM) by oocytes was measured after pre-injecting 50 nL of 50 μM dotinurad (closed circles) or water (open circles) for 20 min.

The data were fitted to the Michaelis-Menten equation to obtain the kinetic parameters described in the Method section and are shown by Eadie-Hofstee plot. All lines were estimated from the kinetic parameters obtained using a nonlinear least-squares regression analysis. Each point represents the mean ± SD.

DMD Fast Forward. Published on August 29, 2023 as DOI: 10.1124/dmd.123.001412
This article has not been copyedited and formatted. The final version may differ from this version.

Figure 4. Effect of intracellular uricosuric agents on the exchange efflux of nicotinic acid (NA) with extracellular UA.

(A, B) Effect of intracellular uricosuric agents on NA efflux by URAT1. The efflux of [^{3}H]NA by water-injected or URAT1-expressing oocytes was measured in the absence (open columns) or presence (closed columns) of extracellular 2 mM UA for 120 min after pre-injecting 50 nL of 100 μM [^{3}H]NA with or without (control) uricosuric agents (50 μM dotinurad, 5 mM lesinurad, 250 μM benzbromarone, 500 μM probenecid). (C) Effect of intracellular uricosuric agents on UA uptake. The uptake of [^{14}C]UA (2 mM) by water-injected or URAT1-overexpressing oocytes was measured for 30 min after pre-injecting 50 nL of 100 μM NA in the absence (control, gray column) and presence of uricosuric agents (50 μM dotinurad, 5 mM lesinurad, 250 μM benzbromarone, 500 μM probenecid, blank columns).

Each point represents the mean ± SD. *: Significantly different from the corresponding 2 mM UA (-) group (A, B) or water group (C) by Student's t-test ($p < 0.05$). †: Significantly different from the 2 mM UA (-) of water group (A, B) by Student's test; from the control of URAT1 group (C) by Dunnett's test ($p < 0.05$).

Figure 5. Uptake of dotinurad by rat kidney slices.

The uptake of dotinurad (100 nM) by rat kidney tissue slices was measured in the absence (open circles) or presence (closed squares) of 1 mM probenecid for 5, 15, 30 and 60 min at 37°C.

DMD Fast Forward. Published on August 29, 2023 as DOI: 10.1124/dmd.123.001412
This article has not been copyedited and formatted. The final version may differ from this version.

Each point represents the mean ± SD from 3 slices. Student's t-test: *$p < 0.05$, compared with control.

DMD Fast Forward. Published on August 29, 2023 as DOI: 10.1124/dmd.123.001412
This article has not been copyedited and formatted. The final version may differ from this version.

Table 1. Estimated IC_{50} values of uricosuric agents on uptake of UA.

IC_{50} (Oocyte)	Co	Pre + Co	Pre + Co / Co ratio
Dotinurad (nM)	24.5 ± 1.3	11.0 ± 1.7	0.45
Lesinurad (μM)	88.2 ± 11.1	52.7 ± 6.6	0.60
Benzbromarone (nM)	329 ± 64	355 ± 58	1.08
Probenecid (μM)	326 ± 58	293 ± 44	0.90
IC_{50} (MDCK-II)	Co	Pre + Co	Pre + Co / Co ratio
Dotinurad (nM)	79.8 ± 11.1	33.2 ± 3.4	0.42
Lesinurad (μM)	32.8 ± 3.4	11.0 ± 1.3	0.34
Benzbromarone (nM)	530 ± 69	631 ± 145	1.19
Probenecid (μM)	288 ± 39	411 ± 68	1.43

Each number represents the mean ± SEM (n = 7 - 14 for oocytes, n = 3 - 4 for MDCK-II cells) obtained by non-linear least-squares regression analysis using KaleidaGraph version 4.0 based on the results shown in Figure 1.

DMD Fast Forward. Published on August 29, 2023 as DOI: 10.1124/dmd.123.001412
This article has not been copyedited and formatted. The final version may differ from this version.

Table 2. Kinetic parameters (K_m, V_{max} and K_i) of *cis*- and *trans*-inhibitory effects of dotinurad on uptake of UA by URAT1

	Dotinurad (nM)	K_m (μM)	V_{max} (pmol/60min/oocyte)	K_i (nM)
Cis-inhibition	0	223 ± 35	28.5 ± 1.6	-
	20	382 ± 61	32.6 ± 2.2	29.1 ± 3.9
	40	475 ± 94	35.9 ± 3.3	28.6 ± 3.1
	80	805 ± 185	43.3 ± 5.6	24.1 ± 1.6
	Dotinurad (μM)	K_m (μM)	V_{max} (pmol/20min/oocyte)	K_i (μM)
Trans-inhibition	0	93.3 ± 7.5	22.9 ± 0.50	-
	50	113 ± 17	9.93 ± 0.44	32.5 ± 0.90

Each number represents the mean ± SEM (n = 9–10) obtained by non-linear least-squares regression analysis using KaleidaGraph version 4.0 based on the results shown in Figure 3.

Figure 1

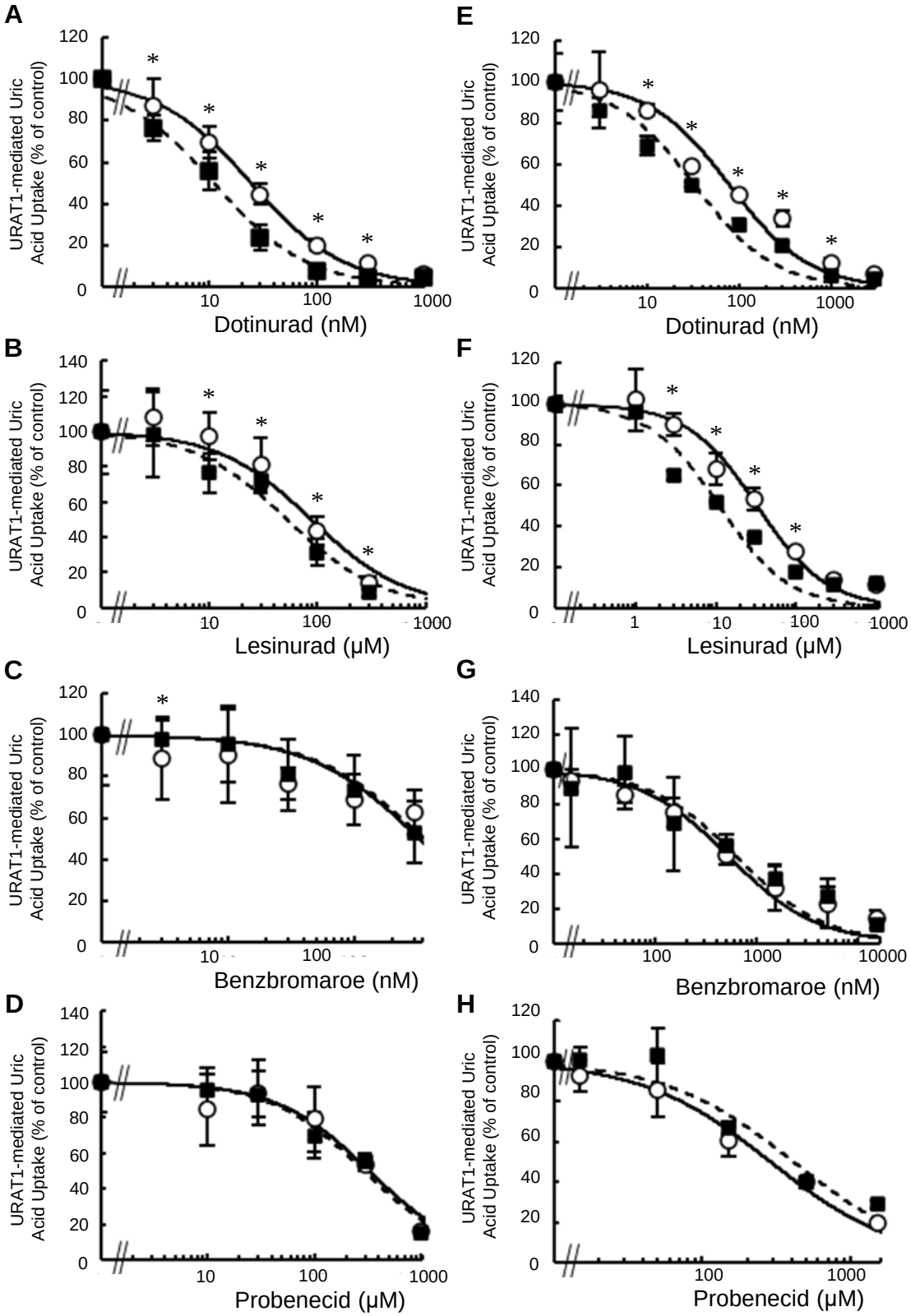

DMD Fast Forward. Published on August 25, 2023 as DOI: 10.1124/dmd.123.001412

Figure 2

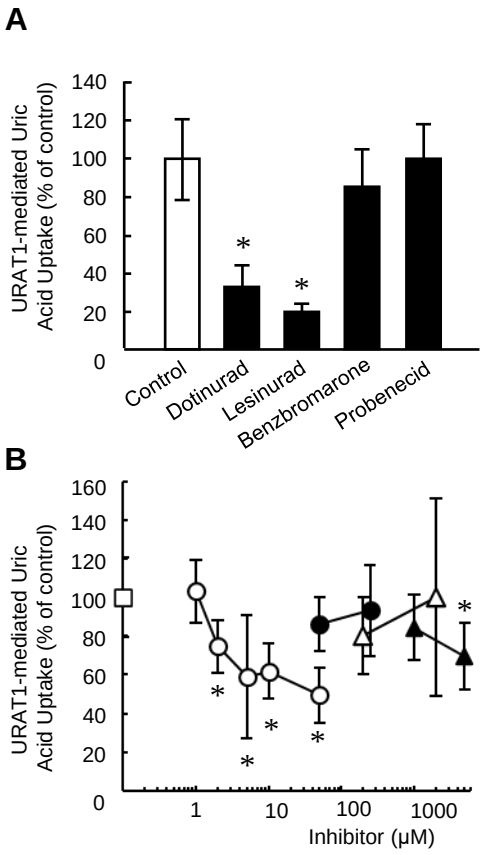

Figure 3

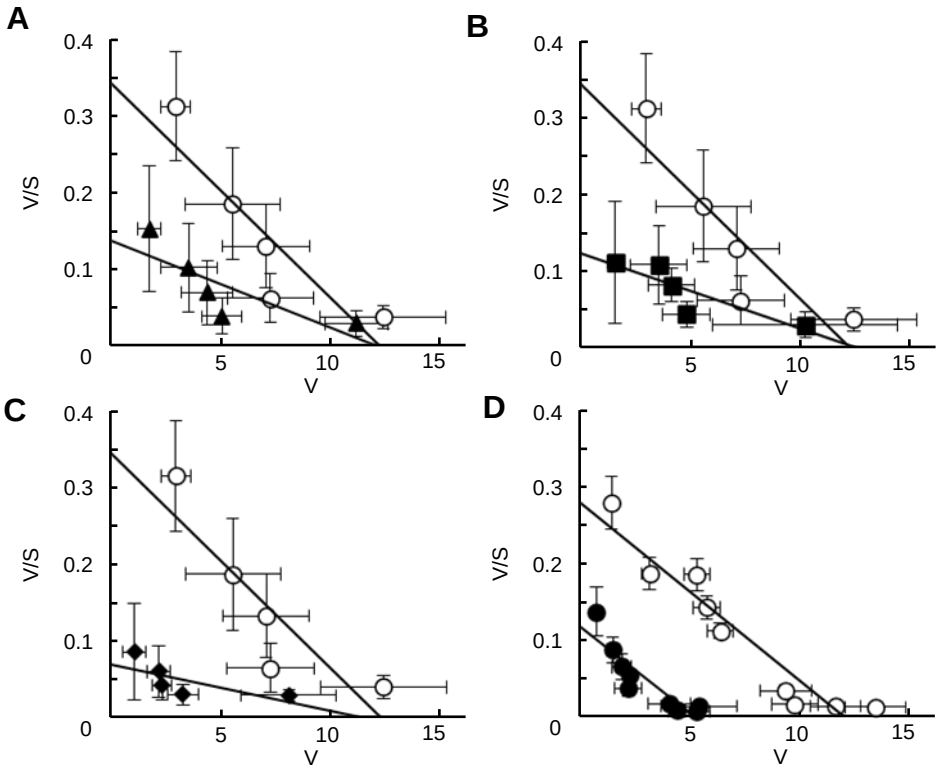

DMD Fast Forward. Published on August 25, 2023 as DOI: 10.1124/dmd.123.001412

Figure 4

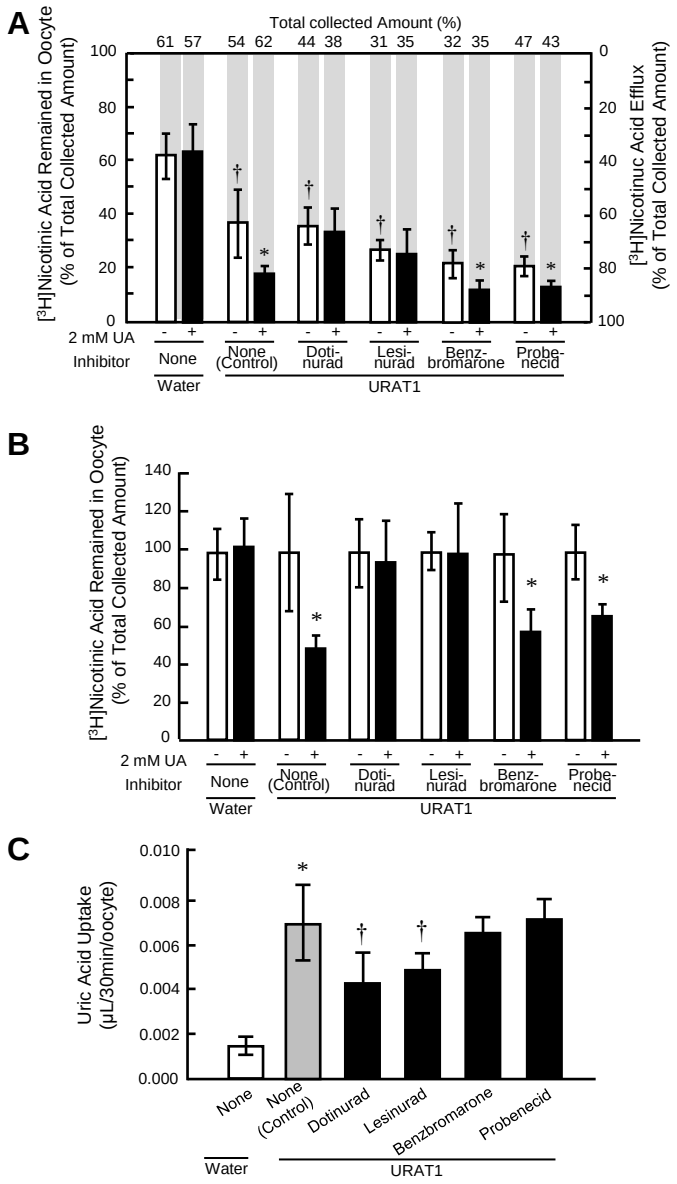

DMD Fast Forward. Published on August 25, 2023 as DOI: 10.1124/dmd.123.001412

Figure 5